This is an accepted version of the article: Mikula, J., and Kulich, M. (2022). **{Triangular Expansion Revisited: Which Triangulation Is The Best?}**. *Proceedings of the 19th International Conference on Informatics in Control, Automation and Robotics - ICINCO*, 313–319, which has been published in a final form at https://doi.org/10.5220/0011278700003271.

Triangular Expansion Revisited: Which Triangulation Is The Best?

Jan Mikula[1,2][a], Miroslav Kulich[2][b]

[1] *Department of Cybernetics, Faculty of Electrical Engineering, Czech Technical University in Prague, Karlovo náměstí 13, 121 35 Praha 2, Czech Republic*

[2] *Czech Institute of Informatics, Robotics and Cybernetics, Czech Technical University in Prague, Jugoslávských partyzánů 1580/3, 160 00 Praha 6, Czech Republic*

{*jan.mikula, miroslav.kulich*}*@cvut.cz*

Keywords: Autonomous Agents, Visibility Region, Triangular Expansion Algorithm, Triangulation, TriVis.

Abstract: Visibility region is a classic structure in computational geometry that finds use in many agent planning problems. *Triangular expansion algorithm* (TEA) is the state-of-the-art algorithm for computing visibility regions within polygons with holes in two dimensions. It has been shown that it is two orders of magnitude faster than the traditional *rotation sweep algorithm* for real-world scenarios. The algorithm triangulates the underlying polygon and recursively traverses the triangulation while keeping track of the visible region. Instead of the *constraint Delaunay triangulation* used by default, this paper introduces the idea of optimizing the triangulation to minimize the expected number of triangle edges expanded during the TEA's traversal while assuming that every point of the input polygon is equally likely to be queried. The proposed triangulation is experimentally evaluated and shown to improve TEA's mean query time in practice. Furthermore, the TEA is modified to consider limited visibility range of real-life sensors. Combined with the proposed triangulation, this adjustment significantly speeds up the computation in scenarios with limited visibility. We provide an efficient open-source implementation called *TriVis* which, besides the mentioned, includes determining visibility between two points and other useful visibility-related operations.

1 INTRODUCTION

Visibility is a fundamental concept in computational geometry, security, and mission planning for mobile robots. In general, we say that a point is visible by an agent from its configuration if the agent is physically capable of seeing the point. All points visible from that particular configuration form a visibility region. Visibility regions are useful when one needs to guard an art gallery by a set of static observers (O'Rourke, 1987), establish a watchman's route from which the whole boundary or interior of an area is visible (Ntafos, 1992; Mikula and Kulich, 2022), or provide a guarantee that a room is free of intruders (Guibas et al., 1997). The classic formulation assumes the configuration is a point in polygon with holes $\mathcal{W} \subset \mathbb{R}^2$, also called *polygonal domain* or *polygonal map*, and two points $q, p \in \mathcal{W}$ are visible to each other if segment $\overline{qp} \subset \mathcal{W}$. The visibility region usually takes the form of star-shaped polygon, but in some exceptional cases, the polygon can have attached one-dimensional antennae (Bungiu et al., 2014). However, the antennae can be often neglected; thus, visibility region $\mathcal{V}(q) \subset \mathcal{W}$ is frequently denoted just as *visibility polygon*.

Although computing visibility polygon $\mathcal{V}(q)$ for given query point $q \in \mathcal{W}$ can be done in polynomial time, frequent employment of this computation as a sub-routine in algorithms often solving NP-hard problems (such as those mentioned earlier) causes the immense need for an efficient implementation. The current state of the art is the *triangular expansion algorithm* (TEA) by (Bungiu et al., 2014). TEA's worst-case query time complexity is $O(n^2)$, where n denotes the number of $\mathcal{W}$'s vertices. However, the authors show that in real-world scenarios the TEA can be by two orders of magnitude faster than the *rotational sweep algorithm* (RSA) by (Asano, 1985) which runs in $O(n \log n)$ in the worst case. The reason is that basic operations performed by the TEA are extremely fast compared to the RSA's, and the polygonal map on which TEA actually runs in $O(n^2)$ has a unique structure quite dissimilar to practical scenarios.

The TEA is based on a simple idea of triangulating the underlying polygonal map in a preprocess-

[a] https://orcid.org/0000-0003-3404-8742
[b] https://orcid.org/0000-0002-0997-5889

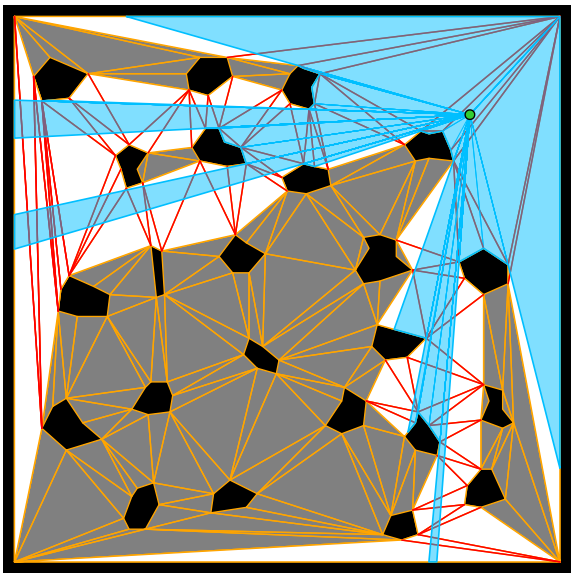

Figure 1: An example of a visibility region computed by the TEA. Borders and holes of the input polygon $\mathcal{W}$ are black. The query point q is green. Triangle edges (not) expanded by the TEA are (orange) red. (Un)visited triangles are (gray) white. The restricted views around q are translucent blue and form the output visibility polygon $\mathcal{V}(q)$.

ing phase and then using the triangulation structure in the query phase to find requested visibility regions. Having the structure, TEA's answer to a query starts by locating triangle $\triangle_q$ containing the query point q. This can be done by a simple walk, as the authors suggest. A recursive procedure is then initiated by expanding the view of q through every edge e_i, $i \in \{1,2,3\}$, of $\triangle_q$ to the neighboring triangle (unless e_i is part of $\mathcal{W}$'s border) and restricting the view by e_i's endpoints. As the recursion proceeds only the edges that are at least partially in the current restricted view are expanded and the view can be further restricted by the endpoints of next expanded edges. A branch of the recursion ends when either all edges that are candidates for expansion are part of the $\mathcal{W}$'s border or the restricted view angle is reduced to zero (may lead to creating an antenna). After all branches of the recursion have ended, the resulting $\mathcal{V}(q)$ is the collection of all the restricted views around q acquired up to that time. See Figure 1 for illustrations of some of these concepts.

TEA's query time is clearly proportional to the number of edge expansions η during the computation of $\mathcal{V}(q)$. In some sense, the TEA is output-sensitive because η partially depends on the complexity of the output, but as the authors state, not strictly because the algorithm may traverse an edge even though the edge does not contribute to the boundary of $\mathcal{V}(q)$ (Bungiu et al., 2014). Preprocessing, i.e., constructing the triangulation of $\mathcal{W}$, can be done at best in $O(n \log n)$ by efficient construction of the *constraint Delaunay triangulation* (CDT) as suggested by (Shewchuk, 2002), although TEA's authors use a CDT implementation that runs in $O(n^2)$. The TEA will work correctly with any valid triangulation. However, the influence of particular triangulation choice on η and thus TEA's query time has escaped researchers' attention so far. Yet, assuming every point in $\mathcal{W}$ is equally likely to be queried, it can be shown that certain triangulations are less or more suited for usage in the TEA than others.

The best triangulation is clearly the one minimizing the expected (mean) number of edge expansions during the progress of the algorithm. In this paper, we design a simple heuristic procedure to obtain a good approximation of such triangulation. The proposed procedure is run on several benchmark instances to obtain the new type of triangulation for each. These triangulations are then experimentally evaluated in the query phase of the TEA and compared to the CDT shown to significantly reduce mean number of expansions $\bar{\eta}$ and thus mean query times for all studied cases and one million random query points.

This work does *not* evaluate TEA's preprocessing time, significantly increased by the triangulation optimization, which is partially caused by a naive implementation of some of its sub-procedures. Instead, the primary purpose of this work is to draw attention to the interesting observation that the particular triangulation matters to TEA's query times.

Overall, the contribution of this work is three-fold.

1. We propose a new type of triangulation to improve TEA's query time,
2. modify the TEA to efficiently cope with more realistic visibility regions, and lastly,
3. provide an efficient open-source TEA's implementation tailored for some of the most common visibility-related tasks, e.g., computing visibility regions, finding all $\mathcal{W}$'s vertices visible from q, and determining visibility between two queries.

2 PROBLEM DEFINITION

In this section, we formalize the search for a triangulation that approximately minimizes the expected number $\bar{\eta}$ of edge expansions done by the TEA while assuming that query points are drawn from a known probability distribution. The approximation is based on a further assumption that the number of edge expansions η is the same as that of expanded edges μ. In general, the assumption is not valid because TEA can expand some triangle edges more than once. (See Figure 1, where the six left-most expanded (red)

edges are actually expanded twice because they are visible through two of the (blue) restricted views.) However, as we show in our experiments, the assumption makes a good approximation because in real-world scenarios the two values are similar, i.e., $\eta \sim \mu$.

Note that exactly those triangle edges that are (at least partially) visible from query point q but do not contribute to the boundary of $\mathcal{W}$ are expanded by the TEA (see Figure 1). Therefore, the number of edges expanded by the TEA at least once given query point q and triangulation $\mathcal{T}$ can be computed as

$$\mu(q,\mathcal{T}) = \sum_{e \in E(\mathcal{T}) : e \notin \partial\mathcal{W}} \mathit{Visible}(e,q), \qquad (1)$$

where $E(\mathcal{T})$ denotes the set of $\mathcal{T}$'s edges, $\partial\mathcal{W}$ the border of $\mathcal{W}$, and

$$\mathit{Visible}(\overline{uv},q) = \begin{cases} 1 & \text{if exists any } p \in \overline{uv} \\ & \text{visible from } q, \\ 0 & \text{else.} \end{cases} \qquad (2)$$

Let the location of the query point be described by random variable Q with a known two-dimensional *probability density function* (PDF). Then, the expected number of expanded edges is given by

$$\bar{\mu}(\mathcal{T}) = \sum_{e \in E(\mathcal{T}) : e \notin \partial\mathcal{W}} P(\mathit{Visible}(e,Q) = 1), \qquad (3)$$

where $P(\mathit{Visible}(e,Q) = 1)$ is the probability that segment e is visible from the point value taken by Q. The optimal triangulation $\mathcal{T}^\star$ is the one minimizing $\bar{\mu}(\mathcal{T})$, i.e.,

$$\mathcal{T}^\star = \operatorname*{arg\,min}_{\mathcal{T} \in \mathcal{T}(\mathcal{W})} \bar{\mu}(\mathcal{T}), \qquad (4)$$

where $\mathcal{T}(\mathcal{W})$ denotes the set of all possible triangulations of $\mathcal{W}$.

Let us further assume that every point in $\mathcal{W}$ is equally likely to be queried. This assumption known in the literature as the *principle of indifference* (Keynes, 1921) implies modeling the query point's location by random variable Q following PDF that is uniform inside $\mathcal{W}$ and zero outside. This yields a specific formula for computing the probability of segment e being visible from the value taken by Q:

$$P(\mathit{Visible}(e,Q) = 1) = \frac{\mathit{Area}(\mathcal{V}(e))}{\mathit{Area}(\mathcal{W})}, \qquad (5)$$

where $\mathit{Area}(\mathcal{V}(e))$ is the area of a region visible from e, and $\mathit{Area}(\mathcal{W})$ is the area of the whole polygonal map. An example of region $\mathcal{V}(e)$ visible from segment e is shown in Figure 2. Substituting (5) into (3) and the result into (4) while removing the constant factor $1/\mathit{Area}(\mathcal{W})$ from the optimization, we get

$$\mathcal{T}^\star = \operatorname*{arg\,min}_{\mathcal{T} \in \mathcal{T}(\mathcal{W})} \left\{ \sum_{e \in E(\mathcal{T}) : e \notin \partial\mathcal{W}} \mathit{Area}(\mathcal{V}(e)) \right\}. \qquad (6)$$

We call the resulting $\mathcal{T}^\star$ *minimum visibility triangulation* (MinVT).

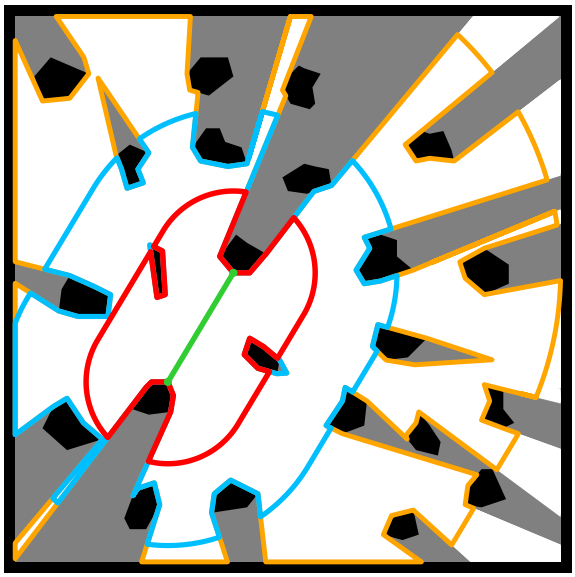

Figure 2: Regions visible from segment e while assuming different maximal visibility ranges. Borders and holes of the input polygon $\mathcal{W}$ are black. Segment e is green. The region visible from e is white, while the unvisible part of $\mathcal{W}$ is gray. Borders of the d-visible regions for restricted visibility ranges $d = 3$, 6, and 12 meters are red, blue, and orange, respectively.

3 SOLUTION APPROACH

3.1 Constructing the New Triangulation

Finding the MinVT is a special case of finding a triangulation minimizing the sum of values (weights) on its edges; a problem known as the *minimum weight triangulation* (MWT), which is NP-hard for a general set of points on a plane and arbitrarily defined weights (Mulzer and Rote, 2008). For the proposed MinVT, the weight of candidate edge e is $w(e) = \mathit{Area}(\mathcal{V}(e))$ (see (6)).

Unlike the triangulation of a set of points, a triangulation of polygonal map $\mathcal{W}$ always contains the edges that contribute to the boundary of $\mathcal{W}$. In addition, a segment is an edge candidate only if its endpoints are vertices of $\mathcal{W}$ and are visible to each other. Although there are known methods for computing the MWT of a simple (without holes) polygon $\mathcal{P}$ (Grantson et al., 2008), the MWT of a polygon with holes $\mathcal{W}$ was not yet addressed in the literature. Therefore, we approximate the MWT of $\mathcal{W}$ by an iterative improvement of its CDT. Starting with $\mathcal{T} \leftarrow \mathrm{CDT}(\mathcal{W})$, in each iteration i, random triangle $\triangle_i \in \mathcal{T}$ is selected first. A simple polygon $\mathcal{P}_i$ is then generated from $\triangle_i$ by gradually adding random adjacent triangles from $\mathcal{T}$. The process of forming $\mathcal{P}_i$ is finished when no triangle can be added to it, i.e., when adding an arbitrary triangle violates simplicity of the

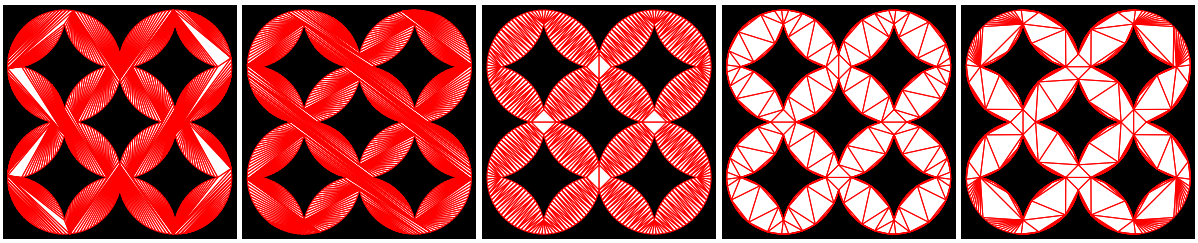

(a) MaxVT (b) MaxLT (c) CDT (d) MinLT (e) MinVT

Figure 3: Different triangulations of the same input polygon ordered according to their (increasing) efficiency in the TEA.

polygon (i.e., adds a hole). Triangles forming $\mathcal{P}_i$ are then substituted in $\mathcal{T}$ by the MWT of $\mathcal{P}_i$. This process converges typically in less than 10 iterations.

The MWT of simple polygon $\mathcal{P}$ has a recursive substructure, which allows to employ dynamic programming (Grantson et al., 2008) depicted in Algorithm 1. Assuming that polygon vertices are numbered consecutively around the polygon boundary, i.e., $\mathcal{P} = \langle p_1, \ldots, p_n \rangle$, a tree of weights $W_{i,j}$ of sub-polygons with vertices between p_i and p_j is build starting from triangles and ending when $W_{1,n}$ is determined. Weights of non-trivial sub-polygons defined by pair of indices (i, j) are evaluated considering all possible triangles $\triangle_{i,j,k}$. Each triangle divides the polygon into three parts: the triangle itself, the sub-polygon to the left, and to the right. Weight $W_{i,j}$ is the minimal sum of weights of these parts and k is stored in $K_{i,j}$. The weight of triangle $\triangle_{i,j,k}$ is computed as

$$\mathit{Weight}(\triangle_{i,j,k}) = \tag{7}$$
$$\ldots \begin{cases} 1/2\big(w(\overline{p_i p_j}) + & \text{if } p_i, p_j, p_k \text{ are} \\ \quad w(\overline{p_j p_k}) + & \quad \text{pairwise visible} \\ \quad w(\overline{p_k p_i})\big) & \quad \text{to each other,} \\ \infty & \text{else.} \end{cases}$$

Finally, the MWT of $\mathcal{P}$ is reconstructed from K in linear time. Starting with pair $(1,n)$ we recursively traverse matrix K. In each step, pair (i, j) determines the base of the triangle $\triangle_{i,j,K_{i,j}}$, which is reported and the reconstruction is called subsequently for its edges $(i, K_{i,j})$ and $(j, K_{i,j})$.

The construction procedure described above can be employed to generate various triangulations of input polygon with holes $\mathcal{W}$ depending on the used weights:

- MinVT: $w(e) = \mathit{Area}(\mathcal{V}(e))$,
- MinLT: $w(e) = \mathit{Length}(e)$,
- MaxVT: $w(e) = -\mathit{Area}(\mathcal{V}(e))$,
- MaxLT: $w(e) = -\mathit{Length}(e)$;

see Figure 3 for examples of these triangulations and CDT, all computed on the same input.

Algorithm 1: MWT for simple polygon $\mathcal{P}$.

```
1  Let P = ⟨p_1, ..., p_n⟩.
2  for i = 2, ..., n do
3      W_{i-1,i} ← 0
4  for δ = 2, ..., n-1 do
5      for i = 1, ..., n-δ do
6          j ← i + δ
7          W_{i,j} ← ∞
8          for k = i+1, ..., j-1 do
9              val ← W_{i,k} + W_{k,j} + Weight(△_{i,j,k})
10             if val < W_{i,j} then
11                 W_{i,j} = val
12                 K_{i,j} = k
```

3.2 d-TEA Modification

Visibility regions are a general concept to model agent's ability to visually cover part of the environment in which it operates. So far, we have considered the most idealized case of omnidirectional vision with an unlimited visibility range. However, in real-life applications, visibility regions can be subject to some additional constraints. Take robotics, for example. Although omnidirectional sensors are common in robotics, their resolution over longer distances is limited to finite range d. A straightforward solution, in this case, is to compute the standard visibility region $\mathcal{V}(q)$ by the TEA and then intersect the result with a circle of radius d centered in q to obtain region $\mathcal{V}(q,d)$. Nevertheless, if the area of $\mathcal{V}(q,d)$ is much smaller than the area of the original $\mathcal{V}(q)$ this approach is highly inefficient because the TEA expands many edges that do not contribute to the output.

To be more efficient with a limited visibility range, we suggest an early exit strategy for the TEA, called d-TEA. During the recurring procedure, only edges that either are inside or intersect the circle of radius d centered in q are expanded, and those that do not are added to the boundary of output region $\mathcal{V}'(q,d)$. To obtain the requested $\mathcal{V}(q,d) \subset \mathcal{V}'(q,d)$, the circle intersection is computed efficiently by rotating around q utilizing the star shape of $\mathcal{V}'(q,d)$.

map	n	h	x [m]	y [m]	a [m^2]	comment
ar	938	11	45.1	43.7	782	*AR0018SR* (MAI)
c4	632	5	31.6	31.6	623	artificial
de	362	4	25.2	30.8	391	*den312d* (MAI)
dr	864	14	57.2	47.8	692	*dr_dungeon* (MAI)
e1	483	1	18.8	18.9	153	expl. data (sim.)
ec	1126	7	24.4	19.7	212	expl. data (real)
jh	278	9	20.6	23.2	460	real
la	331	35	40.0	40.0	1153	artificial
pb	92	3	133.3	104.9	1504	real
ph	153	23	20.0	20.0	367	artificial
ta	87	2	39.7	46.9	731	real

Table 1: Properties of the polygonal maps.

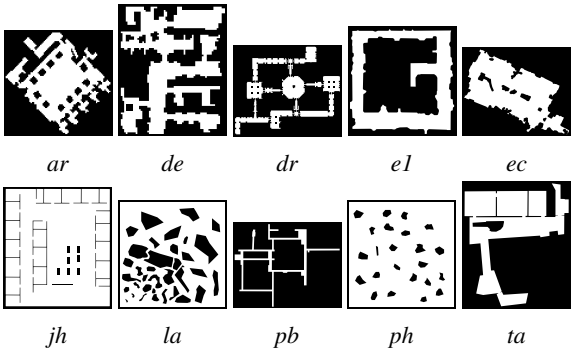

Figure 4: Polygonal maps used in the experiments.

Although the extension from TEA to d-TEA may seem trivial, we need to contemplate that the proposed early exit strategy directly affects how many edges are expanded by the algorithm and thus also the criterion optimized when constructing the proposed triangulation MinVT. The best triangulation for TEA may not be the same for d-TEA with various values of d. Therefore, we need to adapt MinVT's edge weight $w(e)$ from $Area(\mathcal{V}(e))$ to $Area(\mathcal{V}(e,d))$, where $\mathcal{V}(e,\infty) = \mathcal{V}(e)$ and region $\mathcal{V}(e,d)$ is d-visible from segment e for $d \in (0,\infty)$. d-visibility extends the concept of visibility, whereas two points are visible to each other if and only if the line segment between them lies entirely in $\mathcal{W}$ and is no longer than d. Figure 2 shows examples of d-visible regions from particular segment e in $20\,\mathrm{m} \times 20\,\mathrm{m}$ $\mathcal{W}$ for $d = 3$, 6, and 12 meters. Considering d-visibility, the MinVT triangulation is denoted as d-MinVT.

3.3 *TriVis*: The Implementation

C++ implementation of the TEA, d-TEA, and MWT is publicly available along with the data and configuration files that we used in our experiments.[1] The implementation is available in many variants tailored for computing visibility regions, finding all environment vertices that are visible from a query point, or determining visibility between two query points. For computing the CDT, *TriVis* uses *Triangle* (Shewchuk, 1996).

4 EXPERIMENTAL EVALUATION

The proposed triangulation (MinVT) has been evaluated on 11 polygonal maps obtained from various sources. The maps and some of their properties are listed in Table 1. Here, n denotes the number of map's vertices, h the number of its holes, x and y its dimensions, and a its area. Maps *ar*, *de*, and *dr* are based on 2D grid maps from Moving AI (MAI) Lab websites[2] (Sturtevant, 2012) that we converted into polygonal representation. Full names of the MAI maps are in the *comment* column of the table. Maps *e*1, and *ec* are based on mobile robot exploration data (Kulich et al., 2018) obtained from simulation, and real robot, respectively. Maps *jh*, *pb*, *ta*, *la*, and *ph* are robot mission planning benchmarks from which the first three are inspired by real indoor environments, an the last two are artificial. All maps mentioned so far are shown in Figure 4 (not in scale). Finally, *c*4 is the map designed specifically for this paper to manifest differences between the considered triangulations and is shown in Figure 3.

The MinVT, CDT, and the other triangulations discussed in Section 3 have been constructed for all the considered maps. Then, the triangulations were tested in the query phase of the TEA. One million uniformly random query points were generated inside each map, and then visibility regions for all these points were computed by the TEA using the stored triangulations. During the computations, the numbers of expansions were stored and then averaged to obtain metric $\bar{\eta}$. The results in Table 2 show the values of $\bar{\eta}$ and average computational times $\bar{t}$ for all the triangulations and maps. In addition, for the MinVT, the table displays the estimated value of $\bar{\eta}$, $\bar{\mu}$, computed solely from the triangulation (according to (3) and (5)) and the percentage improvement over the CDT ($\bar{\eta}^{\mathrm{CDT}}_{imp}$). The best value of $\bar{t}$ and $\bar{\eta}$ per line is shown in **bold**. Note that all the best values except one value of $\bar{t}$ belong to the MinVT. On average, the MinVT is by 10.6%, and 6.6% more efficient than the CDT, and MinLT, respectively. The results for MaxVT and MaxLT triangulations are the worst, which is not surprising. We evaluated them to show a counterpoint to those good triangulations and emphasize triangulation choice's importance. Since MaxVT

[1] *http://imr.ciirc.cvut.cz/Research/TriVis*

[2] *https://movingai.com/benchmarks/grids.html*

map	MaxVT		MaxLT		CDT		MinLT		MinVT			
	$\bar{t}$ [ns]	$\bar{\eta}$	$\bar{t}$ [ns]	$\bar{\eta}$	$\bar{t}$ [ns]	$\bar{\eta}$	$\bar{t}$ [ns]	$\bar{\eta}$	$\bar{t}$ [ns]	$\bar{\eta}$	$\bar{\mu}$	$\bar{\eta}^{\text{CDT}}_{imp}$ [%]
ar	13,331	299.0	12,167	259.7	10,086	179.3	9,308	173.6	**8,804**	**157.8**	155.5	12.0
c4	10,147	206.3	8,818	175.4	9,019	137.1	7,437	104.3	**5,615**	**99.1**	98.0	27.7
de	3,460	69.5	3,293	63.4	2,888	46.6	2,719	46.1	**2,666**	**43.4**	42.6	6.9
dr	5,338	105.7	5,103	97.3	4,602	72.1	4,232	71.7	**4,123**	**66.0**	64.3	8.5
e1	8,200	185.9	8,087	175.7	7,540	127.4	6,673	119.2	**6,260**	**111.1**	109.6	12.8
ec	30,096	723.6	27,713	620.5	22,590	383.6	19,715	356.3	**18,898**	**336.8**	325.6	12.2
jh	4,299	102.7	4,147	95.6	3,227	60.5	3,126	61.2	**3,027**	**55.2**	52.6	8.8
la	2,957	64.5	2,861	60.0	2,406	42.3	2,303	40.3	**2,245**	**38.4**	37.3	9.3
pb	974	18.1	959	17.6	849	12.5	**817**	12.4	822	**11.8**	11.7	5.3
ph	7,273	180.2	7,207	180.4	5,665	119.0	5,404	113.7	**5,401**	**111.6**	105.1	6.1
ta	1,474	29.9	1,441	28.1	1,339	22.0	1,279	23.1	**1,237**	**20.5**	20.3	7.0

Table 2: Efficiency of computing visibility regions by the TEA with different underlying triangulations.

and MaxLT are not expected to provide any good results, these two triangulations are excluded from further experiments.

Next, we evaluated the remaining triangulations the same way as before but in scenarios with more realistic visibility regions that are constrained by finite visibility range $d \in \{12, 6, 3\}$ m. Limited range d was also considered during the MWT construction as discussed in Section 3.2 in the case of d-MinVT. Therefore, the d-MinVT must have been recomputed for every value of d. The TEA was run in two versions: 1. the standard, and 2. with early exit considering limited visibility range d (recall Section 3.2). The results are shown in Table 3. All values in the table correspond to the metric $\bar{\eta}$ except for the first two columns. We emphasize the four most important observations. First, the early exit strategy helps to reduce the number of expansions for all cases significantly. Second, the proposed d-MinVT triangulation is the best in all cases with early exit as shown in **bold**. Third, since d-MinVT assumes early exit during its own construction, it may not be the best for the standard TEA, as observed in the results. Fourth, the effectiveness of MinLT gets very close to MinVT with smaller visibility ranges. The last observation can be explained using Figure 2. It is apparent that as the visibility range gets smaller, the visible area around segment e is more and more proportionally dependent on the segment's length.

map	d [m]	standard TEA				d-TEA (with early exit)		
		CDT	MinLT	MinVT	d-MinVT	CDT	MinLT	d-MinVT
ar	12	179.3	173.6	157.8	162.9	101.1	95.2	**92.1**
	6				167.8	53.0	49.4	**48.3**
	3				171.6	26.9	24.9	**24.5**
c4	12	137.1	104.3	99.1	104.0	95.4	80.6	**78.6**
	6				107.4	59.3	53.5	**52.6**
	3				105.4	29.2	25.7	**25.5**
de	12	46.6	46.1	43.4	43.8	42.2	41.9	**39.8**
	6				44.9	30.3	30.1	**29.2**
	3				46.2	17.8	17.4	**17.1**
dr	12	72.1	71.7	66.0	66.8	64.5	64.4	**61.4**
	6				69.0	47.3	42.6	**41.6**
	3				71.4	25.1	22.5	**22.2**
e1	12	127.4	119.2	111.1	111.4	119.0	112.0	**105.2**
	6				114.0	83.7	80.5	**77.6**
	3				120.9	46.4	45.2	**43.9**
ec	12	383.6	356.3	336.8	339.7	336.5	314.2	**301.5**
	6				347.6	194.9	181.3	**175.6**
	3				354.7	80.5	73.9	**72.4**
jh	12	60.5	61.2	55.2	55.7	53.2	53.7	**49.3**
	6				58.1	31.6	31.5	**30.0**
	3				59.1	17.0	16.8	**16.4**
la	12	42.3	40.3	38.4	38.9	31.9	31.0	**30.1**
	6				40.1	20.9	20.4	**20.0**
	3				40.6	12.2	11.9	**11.8**
pb	12	12.5	12.4	11.8	12.2	8.0	7.9	**7.8**
	6				12.5	6.1	**6.0**	**6.0**
	3				12.6	4.7	**4.6**	**4.6**
ph	12	119.0	113.7	111.6	112.6	98.3	95.0	**94.0**
	6				113.4	51.6	50.2	**49.7**
	3				113.0	23.9	23.3	**23.1**
ta	12	22.0	23.1	20.5	21.1	17.1	17.9	**16.3**
	6				21.6	11.0	10.8	**10.5**
	3				22.7	6.7	6.2	**6.1**

Table 3: Results for limited visibility range d. All values correspond to the $\bar{\eta}$ metric except for the first two columns.

5 CONCLUSION

We have shown that when computing visibility regions by the *triangular expansion algorithm* (TEA), the choice of the triangulation type matters. Choosing the right or lousy triangulation can shift the average query performance of the TEA significantly in both directions. We have also shown that the *con-*

straint Delaunay triangulation (CDT), although it is commonly used, is not optimal for the TEA in the sense that it does not minimize the expected number of edge expansions done by the algorithm. This paper contributes by designing a new type of triangulation called MinVT that approximately minimizes the above criterion and improves the TEA query performance compared to CDT by about 5-28%, depending on the input map. In addition, the proposed triangulation can adapt to TEA with early exit strategy, called d-TEA, used when computing visibility regions constrained by limited visibility range d.

In future work, we plan to address the preprocessing time, i.e., the time needed for constructing the proposed triangulation, which was not addressed here but appeared slow due to naive approaches used in some of the sub-procedures. Furthermore, a promising direction for future research is generalizing from a triangulation optimization to an optimization of general collection of convex polygons, also called a navigation mesh. A computation similar to TEA's computation of visibility regions but using a general navigation mesh appears in (Shen et al., 2020). Here, Polyanya (Cui et al., 2017), a state-of-the-art optimal solver for computing geometric shortest paths in navigation meshes, was adapted to compute all convex obstacle vertices visible from a query mesh vertex. Adapting the ideas of this paper to navigation meshes used in Polyanya may result in a similar average improvement of query times as for TEA with optimized triangulation.

ACKNOWLEDGMENTS

This work was supported by the European Regional Development Fund under the project Robotics for Industry 4.0 (reg. no. CZ.02.1.01/0.0/0.0/15003/0000470) and by the Grant Agency of the Czech Technical University in Prague, grant No. SGS21/185/OHK3/3T/37.

REFERENCES

Asano, T. (1985). An efficient algorithm for finding the visibility polygon for a polygonal region with holes. *IEICE Transactions*, 68(9):557–559.

Bungiu, F., Hemmer, M., Hershberger, J., Huang, K., and Kröller, A. (2014). Efficient Computation of Visibility Polygons. arXiv:1403.3905.

Cui, M., Harabor, D. D., and Grastien, A. (2017). Compromise-free pathfinding on a navigation mesh. In *Proceedings of the Twenty-Sixth International Joint Conference on Artificial Intelligence, IJCAI-17*, pages 496–502.

Grantson, M., Borgelt, C., and Levcopoulos, C. (2008). Fixed parameter algorithms for the minimum weight triangulation problem. *International Journal of Computational Geometry & Applications*, 18(03):185–220.

Guibas, L. J., Latombe, J.-C., Lavalle, S. M., Lin, D., and Motwani, R. (1997). Visibility-based pursuit-evasion in a polygonal environment. In Dehne, F., Rau-Chaplin, A., Sack, J.-R., and Tamassia, R., editors, *Algorithms and Data Structures*, pages 17–30, Berlin, Heidelberg. Springer Berlin Heidelberg.

Keynes, J. M. (1921). The Principle of Indifference. In *A Treatise on Probability*, volume 4, chapter IV, pages 41–64. Macmillan and Co.

Kulich, M., Kozák, V., and Přeučil, L. (2018). An integrated approach to autonomous environment modeling. In *Modelling and Simulation for Autonomous Systems (MESAS 2017)*, volume 10756 of *Lecture Notes in Computer Vision*. Springer International Publishing AG.

Mikula, J. and Kulich, M. (2022). Towards a continuous solution of the d-visibility watchman route problem in a polygon with holes. *IEEE Robotics and Automation Letters*, 7(3):5934–5941.

Mulzer, W. and Rote, G. (2008). Minimum-weight triangulation is np-hard. *J. ACM*, 55(2).

Ntafos, S. (1992). Watchman routes under limited visibility. *Computational Geometry: Theory and Applications*, 1(3):149–170.

O'Rourke, J. (1987). *Art Gallery Theorems and Algorithms*. Oxford University Press.

Shen, B., Cheema, M. A., Harabor, D., and Stuckey, P. J. (2020). Euclidean pathfinding with compressed path databases. In *Proceedings of the Twenty-Ninth International Joint Conference on Artificial Intelligence, IJCAI-20*, pages 4229–4235.

Shewchuk, J. R. (1996). Triangle: Engineering a 2d quality mesh generator and delaunay triangulator. *Applied Computational Geometry Towards Geometric Engineering*, 1148:203–222.

Shewchuk, J. R. (2002). Delaunay refinement algorithms for triangular mesh generation. *Computational Geometry*, 22(1):21–74.

Sturtevant, N. (2012). Benchmarks for grid-based pathfinding. *Transactions on Computational Intelligence and AI in Games*, 4(2):144 – 148.